Near Resonance Charge Exchange in Ion−Atom Collisions of Lithium Isotopes[†]

Peng Zhang,[‡] Enrico Bodo,[§] and Alexander Dalgarno*,[‡]

Institute for Theoretical Atomic, Molecular and Optical Physics (ITAMP), Harvard-Smithsonian Center for Astrophysics, Cambridge, Massachusetts 02138, and Chemistry Department, "Sapienza" University of Rome, P. A. Moro 5, 00185, Rome, Italy

Received: June 2, 2009; Revised Manuscript Received: August 5, 2009

Collisions of ions and atoms of ^{6}Li and ^{7}Li are explored theoretically over a wide range of energy from 10^{-14} to 1 eV. Accurate ab initio calculations are carried out of the Born−Oppenheimer potentials and the nonadiabatic couplings that are responsible for the near resonance charge exchange. Scattering studies show that the calculated charge exchange cross section follows Wigner's law for inelastic processes for energies below 10^{-10} eV and that the zero temperature rate constant for it is 2.1×10^{-9} cm^3 s^{-1}. At collision energies much larger than the isotope shift of the ionization potentials of the atoms, we show that the near resonance charge exchange process is equivalent to the resonance charge exchange with cross sections having a logarithmic dependence on energy. A comparison with the Langevin model at intermediate energies is also presented.

I. Introduction

Ion−atom collisions are important processes that occur in many physical environments such as plasmas, electrical discharges, planetary atmospheres, and interstellar clouds. The remarkable progress during the past few years in producing, trapping, and controlling cold and ultracold systems including ultracold plasmas,[1] ultracold Rydberg gases,[2,3] and ionization experiments in Bose−Einstein condensates (BECs)[4,5] has made possible the investigation of the role of electric charge in regimes that are dominated by the quantum or classical nature and their overlap. Cold ion−atom collisions have been proposed as means to implement quantum gates,[6] to cool atoms[7,8] and molecules[9,10] lacking closed optical cycles, and to bind small BECs to ions.[11] However, it turns out to be difficult to reach experimentally quantum or semiclassical regimes because of the strong forces produced by stray electric fields on ions. Recently, an observation of a charge exchange reaction between laser-cooled Yb^+ ions in a Paul trap and Yb atoms in a magneto-optical trap has been reported.[12] Rate constants were obtained at collision energies as low as 3 μeV. Good agreement with the Langevin model for resonance charge exchange and theoretical calculations[13] was obtained at energies on the order of millielectronvolts.

The collision of an ion with its neutral parent atom of a different isotopic composition involves elastic and charge exchange processes

$$ {}^aA^+ + {}^bA \rightarrow \begin{cases} {}^aA^+ + {}^bA & \text{(elastic)} \\ {}^aA + {}^bA^+ + \Delta E & \text{(charge exchange)} \end{cases} \tag{1} $$

where the superscripts a and b label the isotopes. Because of the different isotope shifts of the ion and the neutral atom, there is a small energy difference ΔE in the charge exchange process. For the case of HD^+ for which $\Delta E = 3.70 \times 10^{-3}$ eV, we have shown that at energies well above threshold, the scattering can be described by an elastic two-state approximation for which the direct coupling arising from the difference in nuclear masses is neglected.[14] The charge exchange occurs as the particles collide in the lowest $^2\Sigma_g^+$ and $^2\Sigma_u^+$ Born−Oppenheimer (BO) states of the nuclear ion HD^+ and is driven by the difference $\Delta V = V_g(R) - V_u(R)$ between the two potentials. At sufficiently low energies, the inelastic cross section obeys Wigner's law.[15] Theoretically, we believe that this behavior occurs in other similar systems; however, no precise test of the theory has been made beyond HD^+. This is partially due to the difficulties in accurately evaluating the interaction potentials for many-electron systems and more importantly the nuclear-electronic coupling that brings the colliding species asymptotically to the correct limit and enables the charge exchange process.

In the present work, we report our ab initio calculations for charge exchange collisions between the isotopes of ^{6}Li and ^{7}Li ions and atoms, for which the threshold energy ΔE has been well determined both experimentally[16] and theoretically[17] to be 7.47×10^{-5} eV. Because of the relatively small number of electrons involved, an accurate calculation of the interaction potentials and the coupling elements is possible for the system.

II. Theory

We consider ion−atom collisions between ^{6}Li and ^{7}Li with nuclear masses m_6 and m_7. The Hamiltonian after the separation of the kinetic energy operator of the center of nuclear mass (CNM) motion of the total system can be expressed in the body fixed frame as

$$ \hat{H} = \hat{T}_N + \hat{T}_e + \hat{T}_{mp} + V(\mathbf{r}, \mathbf{R}) \tag{2} $$

where $\hat{T}_N$ is the kinetic energy operator for the relative motion of the nuclei, $\hat{T}_{mp}$ is the mass polarization term, $\hat{T}_e$ is the electron kinetic energy, $\mathbf{R}$ is the vector connecting the two nuclei, and $\mathbf{r}$ measures the coordinates of electrons in the CNM frame. By combining $V(\mathbf{r},\mathbf{R})$ with $\hat{T}_e$, we obtain the nonrelativistic BO electronic Hamiltonian

[†] Part of the "Vincenzo Aquilanti Festschrift".

* Corresponding author. E-mail: adalgarno@cfa.harvard.edu.

[‡] Institute for Theoretical Atomic, Molecular and Optical Physics (ITAMP).

[§] "Sapienza" University of Rome.

10.1021/jp905184a
Published on Web 09/11/2009

$$\hat{H}_{\rm el} = \hat{T}_{\rm e} + V(\mathbf{r},\mathbf{R}) = -\frac{\hbar^2}{2m_{\rm e}}\sum_{i=1}^{N_e}\nabla_i^2 + V(\mathbf{r};\mathbf{R}) \quad (3)$$

where $N_{\rm e}$ is the number of electrons in the system and $m_{\rm e}$ is the electron mass. Atomic units will be used throughout the article. At collision energies well below the excited-state energies of the lithium atom and ion, the function space is spanned by the lowest two eigenfunctions of Li_2^+ that separate at large R into combinations of products of lithium atom and lithium ion wave functions. The BO wave functions are of $^2\Sigma_u^+$ and $^2\Sigma_g^+$ symmetry. The 2s $\rightarrow$ 2p transition of Li lies at 1.8 eV.

The mass polarization term reads

$$\hat{T}_{\rm mp} = -\frac{\hbar^2}{2m}\sum_{i,j=1}^{N_{\rm e}}\nabla_i \cdot \nabla_j \quad (4)$$

with $m = m_6 + m_7$ being the total nuclear mass. We write the corresponding matrix element between BO eigenstates $|\alpha\rangle$ and $|\beta\rangle$ as $\varepsilon_{\alpha\beta}^{\rm mp}$. The mass polarization matrix is symmetric, and asymptotically, the two diagonal matrix elements are the same for the g and u states.

The total wave function of the colliding system can be expanded as a sum

$$\Psi^J = e^{iM\varphi}\sum_{\alpha=1}^{2}\frac{1}{R}\chi_\alpha^J(R)\Theta_{M,\Lambda}^J(\vartheta)|\alpha\rangle \quad (5)$$

where J is the total angular momentum, M is its projection, $\Theta_{M,\Lambda}^J(\vartheta)$ is a generalized spherical harmonic, and $\chi_\alpha^J(R)$ describes the radial motion of the nuclei. $\Lambda = 0$ for both BO states. After substituting eq 5 into the time-independent Schrödinger equation, multiplying with $\langle\beta|$, and integrating over the electronic coordinates, we obtain the following set of coupled equations for the radial functions $\chi_\alpha^J(R)$[18,19]

$$\left[-\frac{1}{2\mu}\frac{{\rm d}^2}{{\rm d}R^2} + \varepsilon_\alpha(R) + \frac{\hbar^2}{2\mu R^2}J(J+1) - E\right]\chi_\alpha^J + \sum_\alpha \varepsilon_{\beta\alpha}^{\rm mp}(R)\chi_\alpha^J = \frac{1}{\mu}\sum_{\alpha\neq\beta}\langle\beta|\frac{\partial}{\partial R}|\alpha\rangle\frac{{\rm d}\chi_\alpha^J}{{\rm d}R} + \frac{1}{2\mu}\sum_\alpha\langle\beta|\frac{\partial^2}{\partial R^2}|\alpha\rangle\chi_\alpha^J - \frac{1}{2\mu R^2}\sum_\alpha\langle\beta|\hat{\rm L}_y^2 + \hat{\rm L}_x^2|\alpha\rangle\chi_\alpha^J \quad (6)$$

where $\mu = m_6m_7/(m_6 + m_7)$ is the reduced mass of the system and ε_α is the BO eigenvalue. We define

$$F_{\alpha\beta} = -F_{\beta\alpha} = \langle\alpha|\frac{\partial}{\partial R}|\beta\rangle \quad (7)$$

and

$$V_{\alpha\beta} = \delta_{\alpha\beta}\varepsilon_\alpha + \varepsilon_{\alpha\beta}^{\rm mp} + \frac{1}{2\mu}\langle\alpha|\frac{\partial^2}{\partial R^2}|\beta\rangle - \frac{1}{2\mu R^2}\langle\alpha|\hat{\rm L}_y^2 + \hat{\rm L}_x^2|\beta\rangle \quad (8)$$

where δ is the Kronecker delta. Equation 6 for the nuclear motion at energy $E = k^2/2\mu$ can be written as

$$\left[\mathbf{I}\frac{{\rm d}^2}{{\rm d}R^2} + 2\mathbf{F}\frac{\rm d}{{\rm d}R} + \mathbf{k^2} - \left(\mathbf{I}\frac{J(J+1)}{R^2} + 2\mu\mathbf{V}\right)\right]\chi^J = 0 \quad (9)$$

where $\mathbf{I}$ is the 2×2 identity matrix and $\mathbf{k}^2$ is the diagonal matrix with elements k_α^2 and k_β^2 related to the threshold energy ΔE by

$$k_\beta^2 - k_\alpha^2 = 2\mu\Delta E \quad (10)$$

$\mathbf{F}$ is the first derivative coupling matrix. It has only off-diagonal elements and approaches zero asymptotically in the BO approximation, as we will show in Section III. The matrix $\mathbf{V}$ originates from the radial and angular parts of the nuclear kinetic operator and the mass polarization. The diagonal matrix elements are the adiabatic potentials for the two states, which can be written as

$$V_{\alpha\alpha} = \varepsilon_\alpha^{\rm ad} = \varepsilon_\alpha + \varepsilon_\alpha^{\rm DBOC} \quad (11)$$

The diagonal Born−Oppenheimer correction (DBOC) $\varepsilon_\alpha^{\rm DBOC}$ includes the mass polarization and the second derivative terms from the nuclear kinetic operator.[20−22] The off-diagonal matrix elements couple the two states, and the corresponding eigenvalues separate to the correct limits $\pm^1/_2\Delta E$ asymptotically. It is convenient to write them in Hermitian form as

$$V_{\alpha\beta} = V_{\alpha\beta} - \frac{1}{2\mu}\frac{\rm d}{{\rm d}R}F_{\alpha\beta} + \frac{1}{2\mu}\frac{\rm d}{{\rm d}R}F_{\alpha\beta} = \tilde{V}_{\alpha\beta} + \frac{1}{2\mu}\frac{\rm d}{{\rm d}R}F_{\alpha\beta} \quad (12)$$

$\tilde{V}_{\alpha\beta}$ contains the symmetric combination of the second derivative coupling. The antisymmetric combination results in the second term on the right-hand side of eq 12. Equation 9 has off-diagonal coupling terms asymptotically. The proper scattering boundary conditions can be restored in an atomic representation by addition and subtraction of the two coupled equations of 9, and the resulting equation is similar to eq 9

$$\left[\mathbf{I}\frac{{\rm d}^2}{{\rm d}R^2} + 2\mathbf{F}\frac{\rm d}{{\rm d}R} + \mathbf{k^2} - \left(\mathbf{I}\frac{J(J+1)}{R^2} + 2\mu\mathbf{C}\right)\right]\tilde{\chi}^J = 0 \quad (13)$$

where $\tilde{\chi}_{\alpha,\beta} = \chi_\alpha \pm \chi_\beta$, and the matrix elements of $\mathbf{C}$ are given by

$$C_{\alpha\alpha} = \frac{1}{2}(\tilde{V}_{\alpha\alpha} + \tilde{V}_{\beta\beta}) + \tilde{V}_{\alpha\beta} \quad (14)$$

$$C_{\beta\beta} = \frac{1}{2}(\tilde{V}_{\alpha\alpha} + \tilde{V}_{\beta\beta}) - \tilde{V}_{\alpha\beta}$$

$$C_{\alpha\beta} = \frac{1}{2}(\tilde{V}_{\alpha\alpha} - \tilde{V}_{\beta\beta}) - \frac{\rm d}{{\rm d}R}F_{\alpha\beta}$$

$$C_{\beta\alpha} = \frac{1}{2}(\tilde{V}_{\alpha\alpha} - \tilde{V}_{\beta\beta}) + \frac{\rm d}{{\rm d}R}F_{\alpha\beta}$$

Solutions to eq 13 may be obtained through a modified Numerov algorithm that accounts for the presence of the linear derivative.[14,23,24] The charge exchange and the elastic cross sections can be expressed in terms of the scattering $\mathbf{S}$ matrix as

$$\sigma_{ct}(\alpha \rightarrow \beta) = \frac{\pi}{k_\alpha^2}\sum_J (2J+1)|S^J_{\alpha\beta}|^2 \quad (15)$$

and

$$\sigma_{el}(\alpha \rightarrow \alpha) = \frac{\pi}{k_\alpha^2}\sum_J (2J+1)|1 - S^J_{\alpha\alpha}|^2 \quad (16)$$

respectively. The **S** matrix is obtained in the asymptotic region from the scattering wave function $\tilde{\chi}(R) = \mathbf{J}(R) - \mathbf{N}(R)\cdot\mathbf{K}$ and $\mathbf{S} = (1 + i\mathbf{K})^{-1}\cdot(1 - i\mathbf{K})$, where $\mathbf{J}(R)$ and $\mathbf{N}(R)$ are matrices of the Riccati−Bessel and Riccati−Neumann functions.[25]

In the case of collisions of the same isotopes, all the off-diagonal couplings in eq 13 disappear. Accordingly, resonance charge exchange is related to the two elastic scattering processes with phase shifts η_J^g and η_J^u for the g and u states, respectively, by[26]

$$\sigma_{ct}^{res} = \frac{\pi}{k^2}\sum_{J=0}^{\infty}(2J+1)\sin^2(\eta_J^g - \eta_J^u) \quad (17)$$

and for elastic scattering by

$$\sigma_{el}^{res} = \frac{2\pi}{k^2}\sum_{J=0}^{\infty}(2J+1)\left[\sin^2\eta_J^g + \sin^2\eta_J^u - \frac{1}{2}\sin^2(\eta_J^g - \eta_J^u)\right] \quad (18)$$

Nuclear masses[27] of 6.0151223 and 7.0160040 were used in the calculation.

III. Ab Initio Calculation of BO Potentials and Couplings

A. Born−Oppenheimer Potentials. Ion−atom collisions between the isotopes of Li can be described by two BO potentials, V_g and V_u, which have been previously calculated using model potentials.[28−31] In the present study, we employed the partially spin-restricted open-shell coupled cluster method with singles and doubles[32] and perturbative triples,[33] ROHF-RCCSD(T), and with the correlation-consistent doubly augmented polarized core−valence quintuple-ζ (d-aug-cc-pCV5Z) basis[34] to construct the BO potentials. All electrons were correlated in the coupled cluster calculation. Basis set superposition error (BSSE) was accounted for by the counterpoise procedure.[35] The extra two diffuse functions added in an even-tempered fashion with a factor 2.0 emphasize the long-range interaction, which is critical to the collision dynamics in cold and ultracold conditions. The calculation was carried out between 2.0 and 30.0 bohr radii a_0. The further extension to large distances was achieved by adopting the asymptotic form

$$V_{g,u}(R) \sim V_{dispersion}(R) \pm V_{exchange}(R) \quad (19)$$

with ± for the g and u states, respectively. The dispersion term (in atomic units) was expressed as

$$V_{dispersion}(R) = -\frac{1}{2}\left(\frac{C_4}{R^4} + \frac{C_6}{R^6} + \frac{C_8}{R^8}\right) \quad (20)$$

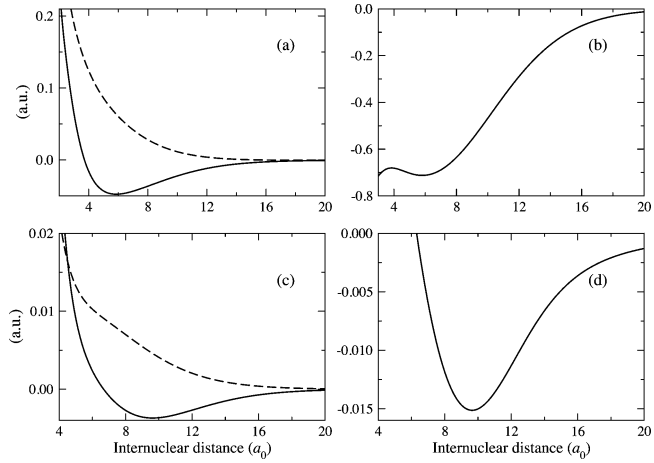

Figure 1. Born−Oppenheimer potentials, first-order derivative coupling F_{01}, and matrix elements of $\tilde{\mathbf{V}}$ as a function of internuclear distances. (a) Solid line is the BO potential of the $^2\Sigma_u^+$ state and dashed line is the $^2\Sigma_g^+$ state. (b) Solid line refers to the first-order derivative coupling F_{01} enlarged by 10^2. (c) Scaled diagonal matrix elements of $\tilde{\mathbf{V}}$, $10^3(\tilde{V}_{00}(R) - \tilde{V}_{00}(\infty))$ (solid line) and $10^3(\tilde{V}_{11}(R) - \tilde{V}_{11}(\infty))$ (dashed line). (d) Scaled off-diagonal matrix elements of $\tilde{\mathbf{V}}$, $10^5(\tilde{V}_{01}(R) - \tilde{V}_{01}(\infty))$.

and the coefficients C_4, C_6, and C_8 are, respectively, the sum of the dipole, quadrupole, and octupole polarizabilities and the corresponding dispersion coefficients. The atomic polarizabilities have been accurately determined by direct variational calculations.[36] They have the values $\alpha_{dipole} = 164.1$, $\alpha_{quadrupole} = 1423$, and $\alpha_{octuple} = 39\,650$. Fitting the calculated ab initio points according to eq 20 yields $C_4 = 164.6$, $C_6 = 1950$, and $C_8 = 79\,300$. The fitted C_4 agrees well with the accurate theoretical value. There are discrepancies between the accurate variational results for C_6 and C_8 and the values derived by ab initio calculations. However, these two terms make little contributions as $R \rightarrow \infty$, where we obtain the **S** matrix by matching the scattering wave function to the standard asymptotic form. The exchange term is extended to large R with the form

$$V_{exchange}(R) = \frac{1}{2}AR^\alpha e^{-\beta R}\left[1 + \frac{B}{R} + \frac{C}{R^2} + O\left(\frac{1}{R^3}\right)\right] \quad (21)$$

with the fitted parameters $A = 0.153$, $\alpha = 2.154$, $\beta = 0.630$, $B = 0.997$, and $C = -9.52$. Bardsley et al.[37] derived a similar asymptotic representation with the parameters $\alpha = 2.177$, $\beta = 0.6295$, $B = 0.519$. The fitted coefficients in eqs 20 and 21 are adopted in our calculations.

The two BO molecular potentials are presented in Figure 1, and the corresponding spectroscopic constants are listed in Table 1 with the available experimental and theoretical values. In general, the agreement is satisfactory. The corrections from BSSE are small, less than 1 cm^{-1} in the whole range of internuclear distances. The larger discrepancies in $\omega_e x_e$ are related to the long-range behavior of the molecular potentials.

B. First Derivative Coupling. The first derivative term in eq 7 couples the $^2\Sigma_g^+$ and $^2\Sigma_u^+$ states when the colliding particles have different nuclear masses. The g and u symmetries of the electronic wave functions are labeled according to the center of charge (CC). The coupling is origin dependent,[18,38,39] and the relationship connecting CNM and CC is given by

$$F_{\alpha\beta} \equiv \langle\alpha|\frac{\partial}{\partial R}|\beta\rangle_{\mathrm{CNM}} = \langle\alpha|\frac{\partial}{\partial R}|\beta\rangle_{\mathrm{CC}} + \frac{\eta m_7 + (\eta - 1)m_6}{m_6 + m_7}\langle\alpha|\nabla_r|\beta\rangle_{\mathrm{CC}}, \quad (22)$$

$$= \langle\alpha|\frac{\partial}{\partial R}|\beta\rangle_{\mathrm{CC}} + \frac{1}{2}\Delta_m\langle\alpha|\nabla_r|\beta\rangle_{\mathrm{CC}}$$

where η is the parameter that determines the origin of the coordinate system and $\Delta_m = (m_7 - m_6)/(m_6 + m_7)$. For the homonuclear diatomic species, $\eta = {}^1/_2$. The first term on the RHS of eq 22 is zero because of the g and u symmetry of the electronic wave functions and the fact that $\langle\alpha|(\partial)/(\partial R)|\alpha\rangle = 0$. The second term is nonzero only if there exists a mass difference between the colliding partners. The evaluation of the first derivative coupling becomes the calculation of the matrix element of the electron velocity operator in the CC frame. We calculated this matrix element using the multiconfiguration self-consistent field (MCSCF) method[40] together with the d-aug-cc-pV5Z basis. The active space in the MCSCF calculation was defined as 5 electrons in 18 molecular orbitals, (5e, 18o), which are composed of the 1s2s2p3s3p atomic orbitals of the Li atom. The accuracy of the method was verified by comparison with the multireference configuration interaction[41] (MRCISD) calculations with the same basis function at selected internuclear distances from 6.0 to 20.0 a_0. The difference is, in general, smaller than 3%. The reference wave function in the MRCISD calculation is the MCSCF(5e,18o) wave function, and all electrons are correlated. The calculated coupling constants as a function of internuclear distance R are depicted in Figure 1.

The asymptotic behavior of $F_{\alpha\beta}$ can be seen by rewriting eq 22 in the length gauge

$$F_{\alpha\beta} = \frac{1}{2}\Delta_m\langle\alpha|\nabla_r|\beta\rangle_{\mathrm{CC}} \approx \frac{1}{2}\Delta_m(\varepsilon_\alpha - \varepsilon_\beta)\langle\alpha|r|\beta\rangle_{\mathrm{CC}} \quad (23)$$

In the BO approximation, it approaches zero as $R \rightarrow \infty$.

C. Diagonal Born−Oppenheimer Correction and Second Derivative Coupling. Effects beyond the BO approximation for many-electron systems are difficult to evaluate accurately because of the cumbersome expressions involved in the separation of the CNM associated with the nuclear kinetic operator and the sensitivity of the small magnitude of those quantities to the quality of the electronic wave functions.[21,42,43] Individual calculation for each of the terms expressed in eq 8 is possible in most quantum chemistry packages except the mass polarization, where an approximation through the resolution identity technique may be introduced. An alternative approach[44−46] is to compute the diagonal terms in the space fixed (SF) frame

$$V_{\alpha\alpha} = \sum_I^{N_{\mathrm{coord}}} \left\langle \alpha \left| -\frac{1}{2m_I}\nabla_I^2 \right| \alpha \right\rangle \quad (24)$$

where the sum is over the number of nuclear Cartesian coordinates N_{coord}, m_I is the nuclear mass and ∇_I^2 is the Laplacian in Cartesian coordinate, I. Such an approach was justified rigorously[47] later, and it has been demonstrated that it has an accuracy of 10^{-4} cm^{-1} for the DBOC of H_2[48] and improves the agreement with experiments for polyatomic molecular systems.[49−51]

We adopted eq 24 in the evaluation of the matrix **V** of eq 8, DBOCs, and the off-diagonal coupling elements. The molecule was placed in the SF nuclear coordinates with the origin at the CNM and the z axis along the molecular axis. The second derivative for each Cartesian coordinate was calculated by numerical differentiation at the MCSCF (5e, 18o) level of theory with the d-aug-cc-pV5Z basis. The close agreement with the MRCISD results in the evaluation of the first derivative coupling element $F_{\alpha\beta}$ indicate that it is an economical approach for the computation of the second derivatives with less severe computational demands. A comparison of $F_{\alpha\beta}$ obtained from numerical differentiation with the directly calculated matrix element of the electron velocity operator serves as a check on the accuracy of the numerical differentiation procedure.

The procedure starts with the calculation of $\tilde{V}_{\alpha\beta}$ as given in eq 12, which is defined as

$$\tilde{V}_{\alpha\beta} = \frac{1}{2}[\langle\alpha|\beta''\rangle + \langle\alpha''|\beta\rangle] \quad (25)$$

where the double primes denote the electronic wave functions differentiated two times with respect to the nuclear coordinate, x. The antisymmetric combination can be readily calculated from the precalculated first derivative coupling

$$\frac{\partial}{\partial x}F_{\alpha\beta} = \frac{1}{2}[\langle\alpha|\beta''\rangle - \langle\alpha''|\beta\rangle] \quad (26)$$

Equations 25 and 26 are obtained by differentiating the orthogonality condition of the BO states. We expand the electronic wave function over the nuclear displacement Δx

$$\alpha(x + \Delta x) = \alpha(x) + \Delta x\alpha'(x) + \frac{1}{2}\Delta x^2\alpha''(x) + \ldots \quad (27)$$

and calculate the BO overlaps

$$O_{\alpha\beta}^{\Delta x} \equiv O_{\alpha\beta}(x, \Delta x) = \langle\alpha(x - \Delta x)|\beta(x + \Delta x)\rangle \quad (28)$$

and

$$O_{\beta\alpha}^{\Delta x} \equiv O_{\beta\alpha}(x, \Delta x) = \langle\beta(x - \Delta x)|\alpha(x + \Delta x)\rangle \quad (29)$$

By substituting eq 27 into eqs 28 and 29 and using a four-point numerical procedure, we obtain

TABLE 1: Spectroscopic Constants, Equilibrium Distance (R_e), Dissociation Energy (D_e), Fundamental Harmonic Vibrational Frequency (ω_e), and Vibrational Anharmonicity ($\omega_e x_e$) of $^7Li_2^+$ (Energy in inverse centimeter, Distance in angstroms)

	R_e	D_e	ω_e	$\omega_e x_e$	ref
$^2\Sigma_g^+$	3.110	10 457.7	261.6	1.47	present
	3.11	10 464(6)	262 ± 2	1.7 ± 5	exptl[56,57]
	3.099	10 441	263.76	1.646	theory[30]
	3.122	10 466	263.08	1.477	theory[31]
$^2\Sigma_u^+$	9.948	88.4	16.63	1.05	present
	9.95	90	20.1	0.13	theory[30]
	10.001	90	16.01	0.79	theory[31]

$$\tilde{V}_{\alpha\beta} = \frac{1}{48\Delta x^2}[16(O_{\alpha\beta}^{\Delta x} + O_{\beta\alpha}^{\Delta x}) - (O_{\alpha\beta}^{2\Delta x} + O_{\beta\alpha}^{2\Delta x}) - 30\delta_{\alpha\beta}] - \vartheta(\Delta x^3) \quad (30)$$

Biorthogonal molecular orbitals at displaced nuclear configurations were used to calculate the BO overlaps.

The derived DBOCs for both states and the coupling element $\tilde{V}_{\alpha\beta}$ are shown in Figure 1. They vary slowly as a function of internuclear distance, R. The asymptotic value of DBOC is 278.13 cm^{-1}. Similar to the BO potentials, DBOCs for both states show minima near the corresponding equilibrium distances of the BO potentials. The asymptotic value of the off-diagonal term, $\tilde{V}_{\alpha\beta}$, is known theoretically. It causes the two adiabatic states to separate to the correct limits of ($^7Li + {}^6Li^+$) and ($^6Li + {}^7Li^+$) with the former lower in energy by $\Delta E = 7.47 \times 10^{-5}$ eV.[16,17] Therefore, $\tilde{V}_{\alpha\beta} = {}^1/_2\Delta E$. The calculated asymptotic value of $\tilde{V}_{\alpha\beta}$, 3.65×10^{-5} eV, agrees closely with the theoretical value of the isotope shift. Field effects and other relativistic contributions[17] are not included in our calculation. For light elements, they are small. To be consistent with the exact separation, the computed $\tilde{V}_{\alpha\beta}$ values were shifted to ${}^1/_2\Delta E$.

The accuracy in the numerical differentiation procedure was checked by comparison of the first derivative coupling, given by

$$F_{\alpha\beta}^{\text{num}} = \frac{1}{4x}(O_{\alpha\beta}^{\Delta x} - O_{\beta\alpha}^{\Delta x}) + \vartheta(\Delta x^2) \quad (31)$$

with the analytical result of $F_{\alpha\beta}$ evaluated by the simple two-point formula. In the whole range of R, the x and y components of $F_{\alpha\beta}^{\text{num}}$ are always smaller than 5.0×10^{-7}, except in the repulsive region of the potentials. The z component is in good agreement with the analytical result. The difference is normally less than ~5%, except in the region of small R, where the numerical noise is large. The relatively large errors in the repulsive region of the potentials cause little change in the scattering calculation because of their small magnitudes compared with the BO potentials and their differences.

The nonadiabatic potential curves obtained by diagonalizing the matrix **V** of eq 8 are presented in Figure 2. With the inclusion of the off-diagonal coupling matrix element, the gerade and ungerade states of Li_2^+ tend to the correct asymptotic limits of ($^7Li^6Li)^+$, separated by the isotope shift ΔE.

The Molpro 2006.1 suite of quantum chemistry programs was used for all electronic structure calculations.[52]

IV. Near Resonance Charge Exchange

Calculations have been carried out for collision energies from 10^{-14} to 1 eV above the ($^6Li + {}^7Li^+$) threshold. The convergence has been carefully examined for the number of partial waves, the integration range, and the integration step length. The computed cross sections are presented in Figure 3. The inelastic exothermic process

$$^6Li + {}^7Li^+ \rightarrow {}^6Li^+ + {}^7Li$$

is described as "quenching" in Figure 3. The cross section behaves as $1/k$, the Wigner threshold law,[15] for energies below 10^{-10} eV. The reverse endothermic excitation process, which is related to the quenching by microscopic reversibility, has a cross section that approaches zero at the threshold ΔE. The elastic cross section tends to a constant.

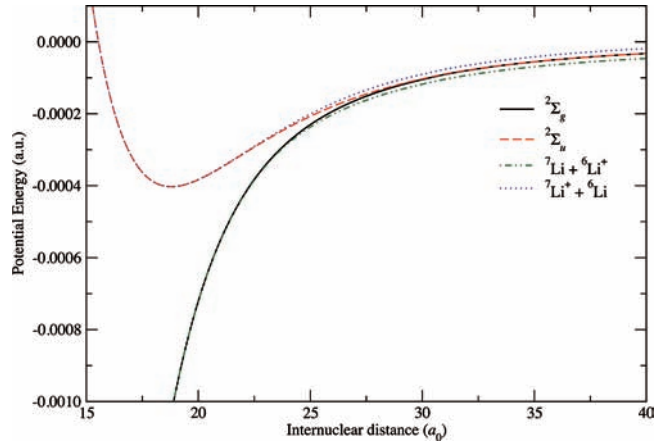

Figure 2. Nonadiabatic potential energy curves of ($^6Li + {}^7Li)^+$ as a function of internuclear distances obtained by diagonalizing the matrix **V** of eq 8. To be visible, the off-diagonal matrix elements of **V** were enlarged by 10 before the diagonalization.

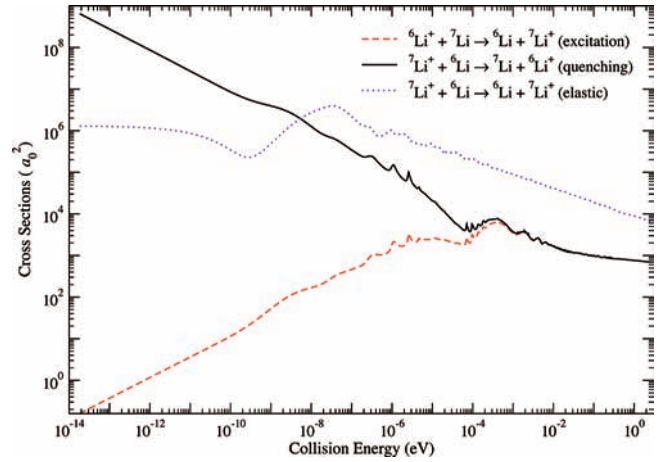

Figure 3. Charge exchange and elastic cross sections for ($^6Li + {}^7Li)^+$ as a function of collision energy above threshold.

TABLE 2: Scattering Length (atomic units) for Near Resonance and Resonance Charge Exchange

	α	β
$^6Li + {}^7Li^+ \rightarrow {}^6Li^+ + {}^7Li$	286	145
	a_g	a_u
$^6Li + {}^6Li^+$	−918	−1425
$^7Li + {}^7Li^+$	14 337	1262

For multichannel scattering, zero energy elastic and inelastic collisions can be described by a complex scattering length,[53] $\alpha - i\beta$, the imaginary part of which is related directly to the inelastic cross section. The derived complex scattering length from the S matrix at low energies is reported in Table 2. In the zero temperature limit, the quenching process has a rate constant of 2.1×10^{-9} cm^3 s^{-1}, which is comparable to the similar quenching process for ion−atom collisions of H with its isotopes.[14] Although the nonadiabatic couplings in the case of Li are weaker than those of H, the smaller energy difference ΔE tends to increase the rate, as has been demonstrated in the case of the hydrogen isotopes. At energies below 10^{-9} eV (~10 μK), the quenching process dominates. Elastic processes prevail otherwise.

Resonance charge exchange (RCE) occurs in an ensemble of mixed isotopes. A comparison of the cross sections for RCE and near resonance charge exchange (NRCE) is presented in

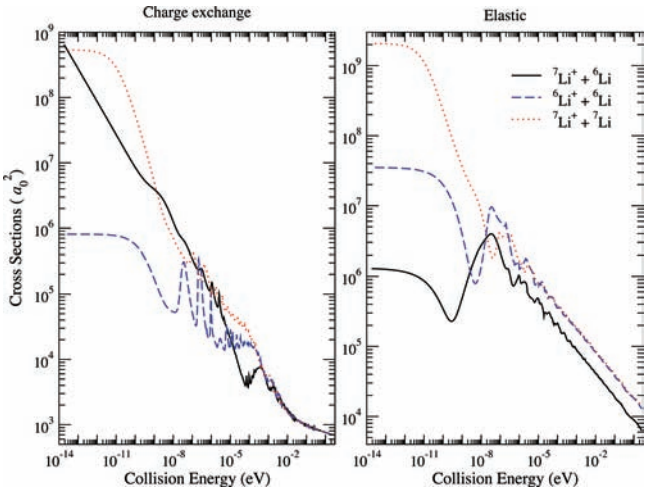

Figure 4. Charge exchange (left) and elastic (right) cross sections of the near resonance and the resonance collisions as a function of collision energy above threshold.

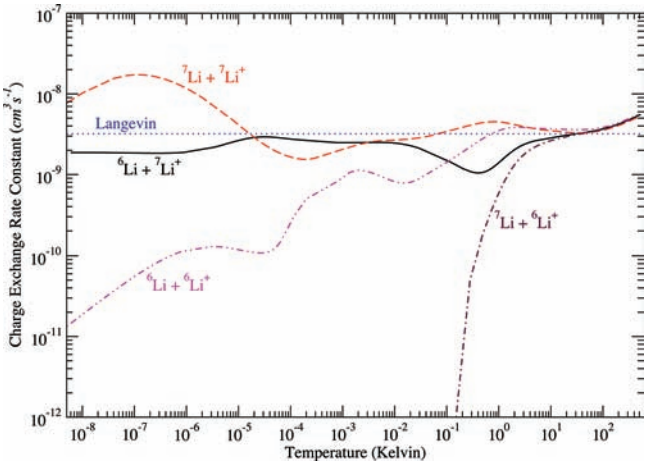

Figure 5. Thermal rate constants of the charge exchange processes for ion−atom collisions of Li isotopes as a function of temperature. The Langevin rate constant is evaluated for the reduced mass of $^6Li + ^7Li^+$.

Figure 4. In the low-energy range ($E < 10^{-9}$ eV), charge exchange is dominated by the large RCE rate of ^7Li shown in Figure 5, where the thermally averaged charge exchange rate constants are plotted as a function of temperature. The enhancement at $\sim 10^{-7}$ K in the rate constant for RCE of ^7Li is a reflection of the behavior of the phase shift difference as the energy approaches zero and depends on the interaction potentials. The smaller RCE cross sections of ^6Li make little contribution to charge exchange in the low-energy regime. The small RCE cross sections of $^6Li^+$ in ^6Li occur because of the similar scattering lengths of the two molecular states.

For collision energies above 10^{-3} eV, which is two orders of magnitude larger than the threshold energy ΔE of $(^6Li^7Li)^+$, the cross sections for the three charge exchange processes are very much the same, varying as $(a \ln E - b)^2$,[54,55] a behavior that reflects the exponential decrease in the exchange energy at large R. Similar behavior was observed in isotopic ion−atom collisions of H.[14] For $(^6Li^7Li)^+$, $a = 1.61a_0$ and $b = 27.8a_0$ with E measured in electron volts and σ_{ct} in units of a_0^2.

In the case of RCE, scattering at ultracold temperatures is characterized by elastic collision processes in the g and u states, respectively. The corresponding scattering lengths a_g and a_u for the g and u states and for ^6Li and ^7Li are reported in Table 2. Both of the elastic processes in the case of RCE have larger cross sections than for NRCE. For energies above 10^{-6} eV, they can be described by the semiclassical expression $(\mu C_4^2/E)^{1/3}$.[54,55]

The Langevin charge exchange model was found to be successful in the intermediate energy range.[13,54,55] The Langevin thermal rate coefficient is independent of temperature and varies weakly with the reduced mass as $\mu^{-1/2}$. It assumes that every collision that surmounts the centrifugal barrier penetrates to small distances and forms a complex that leads to reaction with a probability of order unity. For $^7Li^+$ ions undergoing charge exchange with ^6Li, the Langevin rate coefficient is 3.2×10^{-9} $cm^3\ s^{-1}$.

The quantum mechanical rate coefficient at low energies for the NRCE is also a constant independent of temperature because the cross section varies inversely as the relative velocity. It is determined by s-wave scattering. The s-wave scattering is given by the scattering length, which is sensitive to the details of the interaction potential and to the reduced mass. Figure 5 compares the Langevin formula with quantum mechanical calculations. The quantal rate coefficients undergo small oscillations and are always smaller than the Langevin value until a temperature of ~40 K is reached. A similar level of agreement is found experimentally for charge exchange of Yb^+ ions in Yb atoms by Grier et al.[12] where the threshold energy was estimated to be ~4000 neV, an order of magnitude smaller than that of Li. In Figure 5, we also present the rate coefficients for the reverse reaction of $^6Li^+$ ions in a gas of ^7Li atoms. The forward (k^+) and reverse (k^-) rate coefficients are related by

$$k^+ = k^- e^{-\Delta E/k_B T} \tag{32}$$

The rate coefficients evaluated by eq 32 are consistent with those derived from the computed excitation cross sections.

The charge exchange cross sections in the Wigner and Langevin regimes vary as the inverse of velocity, albeit governed by different physical principles. The rate coefficients in the two regimes could be close because of chance. Therefore, care must be taken when comparing with the Langevin charge exchange rate coefficient.

V. Conclusions

We have investigated ion−atom collisions between the ^6Li and ^7Li isotopes of the lithium atom at low energies. The NRCE is enabled by the coupling of the nuclear and electronic motion, which requires a treatment including adiabatic and nonadiabatic corrections to the BO approximation.

We have performed ab initio calculations to construct the BO potentials and the diagonal and off-diagonal corrections that reflect the breakdown of the BO approximation. We have demonstrated that the NRCE cross section in the low-energy limit follows Wigner's threshold law, varying as the inverse of velocity, and has a large limiting rate constant of 2.1×10^{-9} $cm^3\ s^{-1}$. In comparison, the resonance charge exchange rate goes to zero. When the collision energy is much higher than the threshold energy arising from the isotope shift, NRCE becomes identical to resonance charge exchange. At electron volt energies, the cross sections show a logarithmic dependence on energy. Close agreement with the Langevin charge exchange rate coefficient is found in the intermediate energy range.

Acknowledgment. P.Z. and A.D. acknowledge support from the Chemical Science, Geoscience. and Bioscience Division of the Office of Basic Energy Science, Office of Science, U.S.

Department of Energy. E.B. acknowledges travel support from the Institute for Theoretical Atomic, Molecular, and Optical Physics (ITAMP), which is funded by the NSF and the financial support of "Sapienza", University of Rome. The computational resources were provided by the National Center for Atmospheric Research (NCAR).

References and Notes

(1) Killian, T. C.; Kulin, S.; Bergeson, S. D.; Orozco, L. A.; Orzel, C.; Rolston, S. L. *Phys. Rev. Lett.* **1999**, *83*, 4776.
(2) Mourachko, I.; Comparat, D.; Tomasi, F. d.; Fioretti, A.; Nosbaum, P.; Akulin, V. M.; Pillet, P. *Phys. Rev. Lett.* **1998**, *80*, 253.
(3) Anderson, W. R.; Veale, J. R.; Gallagher, T. F. *Phys. Rev. Lett.* **1998**, *80*, 249.
(4) Kraft, S.; Günther, A.; Fortágh, J.; Zimmermann, C. *Phys. Rev. A* **2007**, *75*, 063605.
(5) Massignan, P.; Bruun, G. M.; Smith, H. *Phys. Rev. A* **2005**, *71*, 033607.
(6) Idziaszek, Z.; Calarco, T.; Zoller, P. *Phys. Rev. A* **2007**, *76*, 033409.
(7) Makarov, O. P.; Côté, R.; Michels, H.; Smith, W. W. *Phys. Rev. A* **2003**, *67*, 042705.
(8) Moriwaki, Y.; Tachikawa, M.; Maeno, Y.; Shimizu, T. *Jpn. J. Appl. Phys., Part 1* **1992**, *31*, 1640.
(9) Smith, W. W.; Makarov, O. P.; Lin, J. *J. Mod. Opt.* **2005**, *52*, 2253.
(10) Mølhave, K.; Drewsen, M. *Phys. Rev. A* **2000**, *62*, 011401(R).
(11) Côté, R.; Kharchenko, V.; Lukin, M. D. *Phys. Rev. Lett.* **2002**, *89*, 093001.
(12) Grier, A. T.; Cetina, M.; Oručević, F.; Vuletić, V. *Phys. Rev. Lett.* **2009**, *102*, 223201.
(13) Zhang, P.; Côté, R.; Dalgarno, A. *Phys. Rev. A*, in press.
(14) Bodo, E.; Zhang, P.; Dalgarno, A. *New J. Phys.* **2008**, *10*, 033024.
(15) Wigner, E. P. *Phys. Rev.* **1948**, *73*, 1002.
(16) Bushaw, B. A.; Nörtershäuser, W.; Drake, G. W. F.; Kluge, H.-J. *Phys. Rev. A* **2007**, *75*, 052503.
(17) Yan, Z.-C.; Nörtershäuser, W.; Drake, G. W. F. *Phys. Rev. Lett.* **2008**, *100*, 243002.
(18) Heil, T. G.; Butler, S. E.; Dalgarno, A. *Phys. Rev. A* **1981**, *23*, 1100.
(19) Grosser, J. *Z. Phys. D: At., Mol. Clusters* **1986**, *3*, 39.
(20) Dalgarno, A.; McCarroll, R. *Proc. R. Soc. London, Ser. A* **1956**, *237*, 383.
(21) Kołos, W.; Wolniewicz, L. *Rev. Mod. Phys.* **1963**, *35*, 473.
(22) Bunker, P. R. *J. Mol. Spectrosc.* **1968**, *28*, 422.
(23) Leroy, J. P.; Wallace, R. *J. Phys. Chem.* **1985**, *89*, 1928.
(24) Tselyaev, V. I. *J. Comp. Appl. Phys.* **2004**, *170*, 103.
(25) Johnson, R. B. *J. Chem. Phys.* **1978**, *69*, 4678.
(26) Mott, N. F.; Massey, H. S. W. *The Theory of Atomic Collisions*, 3rd ed.; Oxford University Press: London, 1965.
(27) NIST, Atomic Weights and Isotopic Compositions. http://physics.nist.gov/PhysRefData/Compositions/.
(28) Dalgarno, A.; Bottcher, C.; Victor, G. A. *Chem. Phys. Lett.* **1970**, *7*, 265.
(29) Bottcher, C.; Allison, A. C.; Dalgarno, A. *Chem. Phys. Lett.* **1971**, *11*, 307.
(30) Schmidt-Mink, I.; Müller, W.; Meyer, W. *Chem. Phys.* **1985**, *92*, 263.
(31) Magnier, S.; Rousseau, S.; Allouche, A. R.; Hadinger, G.; Aubert-Frécon, M. *Chem. Phys.* **1999**, *246*, 57.
(32) Knowles, P. J.; Hampel, C.; Werner, H.-J. *J. Chem. Phys.* **1993**, *99*, 5219.
(33) Watts, J. D.; Gauss, J.; Bartlett, R. J. *J. Chem. Phys.* **1993**, *98*, 8718.
(34) Peterson, K. A., private communication.
(35) Boys, S. B.; Bernadi, F. *Mol. Phys.* **1970**, *19*, 533.
(36) Yan, Z.-C.; Babb, J. F.; Dalgarno, A.; Drake, G. W. F. *Phys. Rev. A* **1996**, *54*, 2824.
(37) Bardsley, J. N.; Holstein, T.; Junker, B. R.; Sinha, S. *Phys. Rev. A* **1975**, *11*, 1911.
(38) Buenker, R. J.; Li, Y. *J. Chem. Phys.* **2000**, *112*, 8318.
(39) Belyaev, A. K.; Dalgarno, A.; McCarroll, R. *J. Chem. Phys.* **2002**, *116*, 5395.
(40) Werner, H.-J.; Knowles, P. J. *J. Chem. Phys.* **1985**, *82*, 5053.
(41) Werner, H.-J.; Knowles, P. J. *J. Chem. Phys.* **1988**, *89*, 5803.
(42) Bardo, R. D.; Wolfsberg, M. *J. Chem. Phys.* **1978**, *68*, 2686.
(43) Lengsfield, B. H., III; Yarkony, D. R. *J. Chem. Phys.* **1986**, *84*, 348.
(44) Sellers, H.; Pulay, P. *Chem. Phys. Lett.* **1984**, *103*, 463.
(45) Handy, N. C.; Yamaguchi, Y.; Schaefer, H. F., III *J. Chem. Phys.* **1986**, *84*, 4481.
(46) Handy, N. C.; Lee, A. M. *Chem. Phys. Lett.* **1996**, *252*, 425.
(47) Kutzelnigg, W. *Mol. Phys.* **1997**, *90*, 909.
(48) Cencek, W.; Kutzelnigg, W. *Chem. Phys. Lett.* **1997**, *266*, 383.
(49) Schwenke, D. W. *J. Chem. Phys.* **2003**, *118*, 6898.
(50) Valeev, E. F.; Sherrill, C. D. *J. Chem. Phys.* **2003**, *118*, 3921.
(51) Gauss, J.; Tajti, A.; Kállay, M.; Stanton, J. F.; Szalay, P. G. *J. Chem. Phys.* **2006**, *125*, 144111.
(52) *MOLPRO*. is a package of ab initio programs written by: Werner, H.-J.; Knowles, P. J.; Lindh, R.; Manby, F. R.; Schütz, M.; Celani, P.; Korona, T.; Mitrushenkov, A.; Rauhut, G.; Adler, T. B.; Amos, R. D.; Bernhardsson, A.; Berning, A.; Cooper, D. L.; Deegan, M. J. O.; Dobbyn, A. J.; Eckert, F.; Goll, E.; Hampel, C.; Hetzer, G.; Hrenar, T.; Knizia, G.; Köppl, C.; Liu, Y.; Lloyd, A. W.; Mata, R. A.; May, A. J.; McNicholas, S. J.; Meyer, W.; Mura, M. E.; Nicklass, A.; Palmieri, P.; Pflüger, K.; Pitzer, R.; Reiher, M.; Schumann, W.; Stoll, H.; Stone, J.; Tarroni, R.; Thorsteinsson, T.; Wang, M.; Wolf, A.
(53) Balakrishnan, N.; Kharchenko, V.; Forrey, R. C.; Dalgarno, A. *Chem. Phys. Lett.* **1997**, *280*, 5.
(54) Côté, R.; Dalgarno, A. *Phys. Rev. A* **2000**, *62*, 012709.
(55) Dalgarno, A. *Philos. Trans. R. Soc. London, Ser. A* **1956**, *250*, 426.
(56) Bernheim, R. A.; Gold, L. P.; Tipton, T. *J. Chem. Phys.* **1983**, *78*, 3635.
(57) Bernheim, R. A.; Gold, L. P.; Tipton, T.; Konowalow, D. D. *Chem. Phys. Lett.* **1984**, *105*, 201.

JP905184A